Choroidal Vascular Flow Area in Central Serous Chorioretinopathy Using Swept-Source Optical Coherence Tomography Angiography

Massimo Nicolò,[1,2] Raffaella Rosa,[1] Donatella Musetti,[1] Maria Musolino,[1] Michela Saccheggiani,[1] and Carlo Enrico Traverso[1]

[1]Clinica Oculistica Università di Genova DINOGMI - IST San Martino IST, Genova, Italy
[2]Fondazione per la Macula onlus, Genova, Italy

Correspondence: Massimo Nicolò, Clinica Oculistica Università di Genova DINOGMI – IRCCS AOU San Martino IST, Viale Benedetto XV, n. 5, Genova, GE 16132, Italy; massimonicolo@gmail.com.

Submitted: January 3, 2017
Accepted: March 6, 2017

Citation: Nicolò M, Rosa R, Musetti D, Musolino M, Saccheggiani M, Traverso CE. Choroidal vascular flow area in central serous chorioretinopathy using swept-source optical coherence tomography angiography. *Invest Ophthalmol Vis Sci*. 2017;58:2002–2010. DOI:10.1167/iovs.17-21417

Purpose. To report the choroidal vascular flow area in eyes with central serous chorioretinopathy (CSC) compared with healthy subjects and unaffected fellow eyes using swept-source (SS) optical coherence tomography (OCT) angiography.

Methods. Prospective case series of 19 eyes of 19 consecutive patients affected by CSC, compared with 15 unaffected fellow eyes and 20 eyes of 10 healthy subjects. Patients underwent SS-OCT angiography in order to evaluate the choroidal vascular flow area of choriocapillaris (CC) and deeper choroidal layers.

Results. The choroidal vascular flow area was higher in eyes with CSC than in control eyes (53.4 ± 5.8% vs. 49.45 ± 8.16%; $P = 0.0001$). Within the choroid of CSC patients choroidal vascular flow area of the CC was significantly lower than the deeper level (50.97 ± 2.8% vs. 54.22 ± 6.3%; $P = 0.025$). There were no differences within the choroid of control eyes. The choroidal vascular flow area at the level of the CC was higher in the unaffected fellow eye (50.74 ± 0.9%; $P = 0.019$) than in control eyes. Choroidal vascular flow area of unaffected fellow eyes did not differ from CSC eyes ($P = 0.17$). The choroidal vascular flow area at the level of the CC was higher in the CSC eyes ($P = 0.0009$) compared with unaffected fellow eyes.

Conclusions. Choroidal vascular flow area is larger in CSC eyes compared with control eyes. However, within the choroid of eyes with CSC, there might be some differences in flow area between CC and deeper choroidal levels. This difference might be secondary to a compensatory mechanism of the choroid.

Keywords: central serous chorioretinopathy, oct angiography, choroid, swept-source

Central serous chorioretinopathy (CSC) is characterized by the development of serous neurosensory retinal detachment at the posterior pole. In the majority of patients, CSC is self-limiting and patients usually have a good visual prognosis. However, in cases of chronic CSC with persistent serous retinal detachment and chronic decompensation of the RPE, progressive visual loss attributable to photoreceptor disruption, and cystoid edema of the neurosensory retina might develop.[1,2]

The increasing use of indocyanine green angiography (ICGA) in CSC has improved the understanding of the pathogenesis of the disease and has demonstrated that during CSC choroidal circulation in addition to RPE is primarily affected, resulting in multifocal areas of choroidal vascular hyperpermeability.[3]

With the clinical introduction of optical coherence tomography (OCT)-angiography, a principally new method has become available to image the macula in a noninvasive manner.[4–7] The purpose of our study was to report the choroidal vascular flow area in eyes with CSC and to compare them with healthy subjects and unaffected fellow eyes.

Methods

Subjects

The institutional review board of the University of Genova IRCCS San Martino IST approved the study protocol and the collection of data related to all the patients affected by CSC. The study was conducted in accordance with the tenets of the Declaration of Helsinki. Written informed consent was obtained from each subject before any study procedures or examinations.

We recruited naïve consecutive patients with nonresolving forms of CSC[8] referred to the Medical Retina Center of the University Eye Clinic of Genova, Italy and visited between May 2016 and September 2016. Central serous chorioretinopathy was defined as chronic when subretinal fluid persisted for 6 months or more. Healthy eyes were recruited from healthy volunteers and unaffected fellow eyes of patients with unilateral CSC disease. All the subjects underwent a comprehensive ocular examination, including autorefractometry, best-corrected visual acuity measurement with Early Treatment Diabetic Retinopathy Study chart, slit-lamp biomicroscopy, IOP

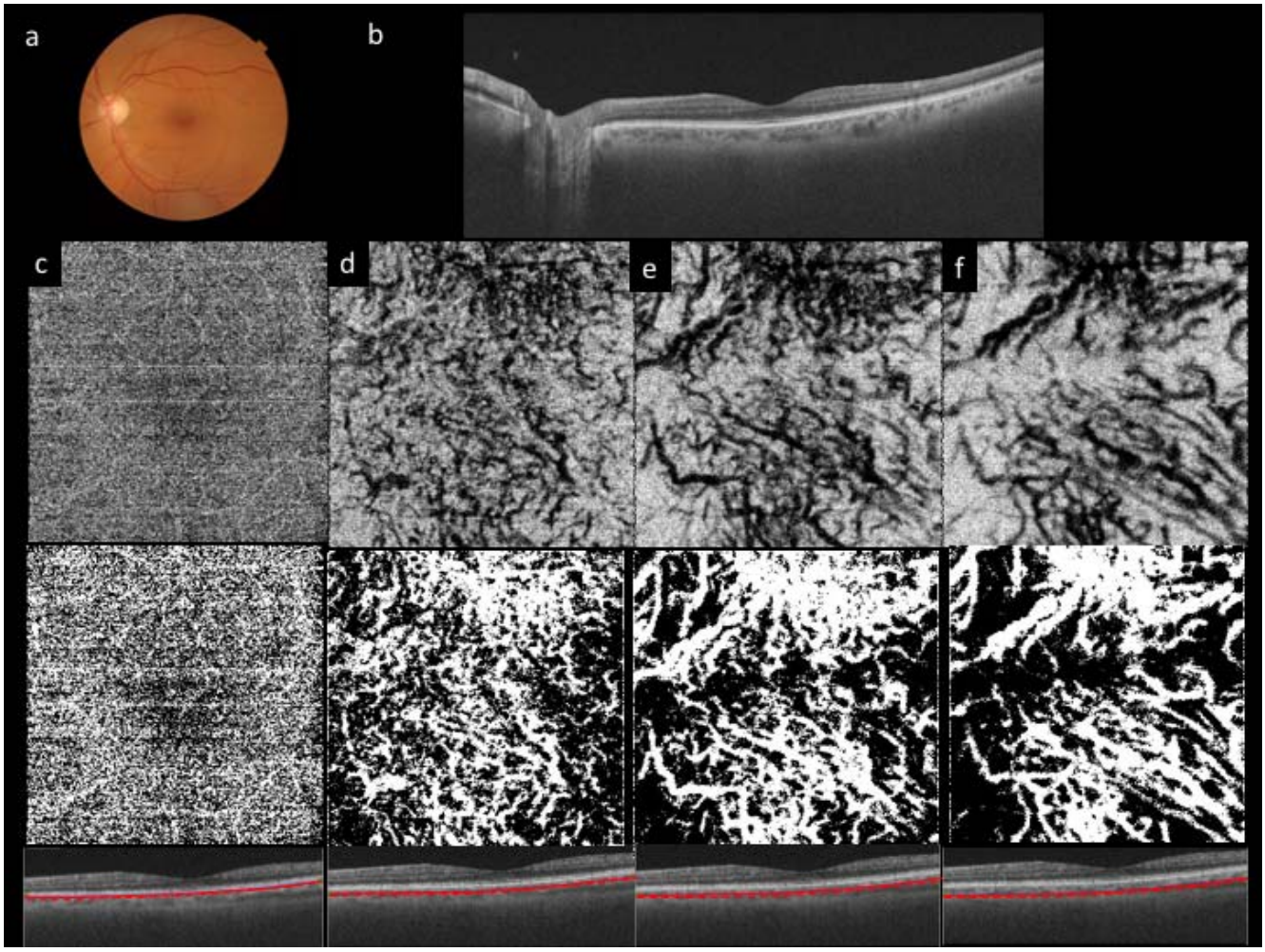

Figure 1. Representative images of a healthy left eye of a 51-year-old man. (**a**) Fundus photograph. (**b**) Horizontal scan by SS-OCT. (**c**) *Upper*: OCTA image 4.5 × 4.5 mm of the microvasculature of the choriocapillaris 10.4-μm external to the Bruch's membrane; (**c**) *middle*: binarized image; (**c**) *bottom*: coregistered B scans showing the position of the segmentation lines. (**d**) *Upper*: OCTA image 4.5 × 4.5 mm of the choroid obtained positioning the segmentation line at 59.6 and 80.6 μm from the Bruch's membrane; (**d**) *middle*: binarized image; (**d**) *bottom*: coregistered B scans showing the position of the segmentation lines. (**e**) *Upper*: OCTA image 4.5 × 4.5 mm of the choroid obtained positioning the segmentation line at 80.6 and 119.6 μm from the Bruch's membrane; (**d**) *middle*: binarized image; (**d**) *bottom*: coregistered B scans showing the position of the segmentation lines. (**f**) *Upper*: OCTA image 4.5 × 4.5 mm of the choroid obtained positioning the segmentation line at 119.6 to 137.8 μm from the Bruch's membrane; (**f**) *middle*: binarized image; (**f**) *bottom*: coregistered B scans showing the position of the segmentation lines.

measurement, and fundus photography. Fluorescein (FA) and ICGA using the Topcon ImageNet System (Tokyo, Japan) were performed only on CSC patients. All patients underwent swept-source (SS)-OCT and SS-OCT angiography imaging (SS-OCTA). Subjects included in the study did not have any additional systemic comorbidity.

Swept-Source Optical Coherence Tomography

The OCT device (DRI OCT Triton; Topcon Corporation) we used in this study has a central wavelength of 1050 nm, an acquisition speed of 100,000 A-scans per second, and an axial and transversal resolution of 7 and 20 μm in tissue, respectively. Swept-source OCT examinations were performed by trained examiners after pupil dilation. Each subject underwent horizontal and vertical line scans (12 mm and 128 averaging), 12 radial line (12 mm) and three-dimensional (3D) macula acquisition protocol centered on the fovea. Each 3D volumetric scan covered an area of 4.5 × 4.5 mm^2 centered on the fovea. Three-dimensional 4.5 × 4.5 mm^2 volumetric scans consisted of 320 (horizontal) × 320 (vertical) A-scans.

Measurement of Choroidal Thickness

Choroidal thickness was defined as the distance between the line corresponding to the Bruch's membrane beneath the RPE and the chorioscleral interface. The Topcon built-in proprietary software ImageNet 6 automatically measured choroidal thickness in the macula region.

Swept-Source Optical Coherence Tomography Angiography

Swept-source OCT angiography scans were taken from 4.5 × 4.5 mm^2 cubes with each cube consisting of 320 clusters of four repeated B-scans centered on the fovea. Angio-OCT images of the choriocapillaris was generated, automatically by the software at the level of the choriocapillaris (CC). The software automatically positions one segmentation line at the level of the Bruch's membrane and the other 10.4-μm external to the first one. Angio-OCT images of three deeper choroidal levels were also obtained moving down the segmentation lines in order to select Sattler and Haller layers. It is reported that the

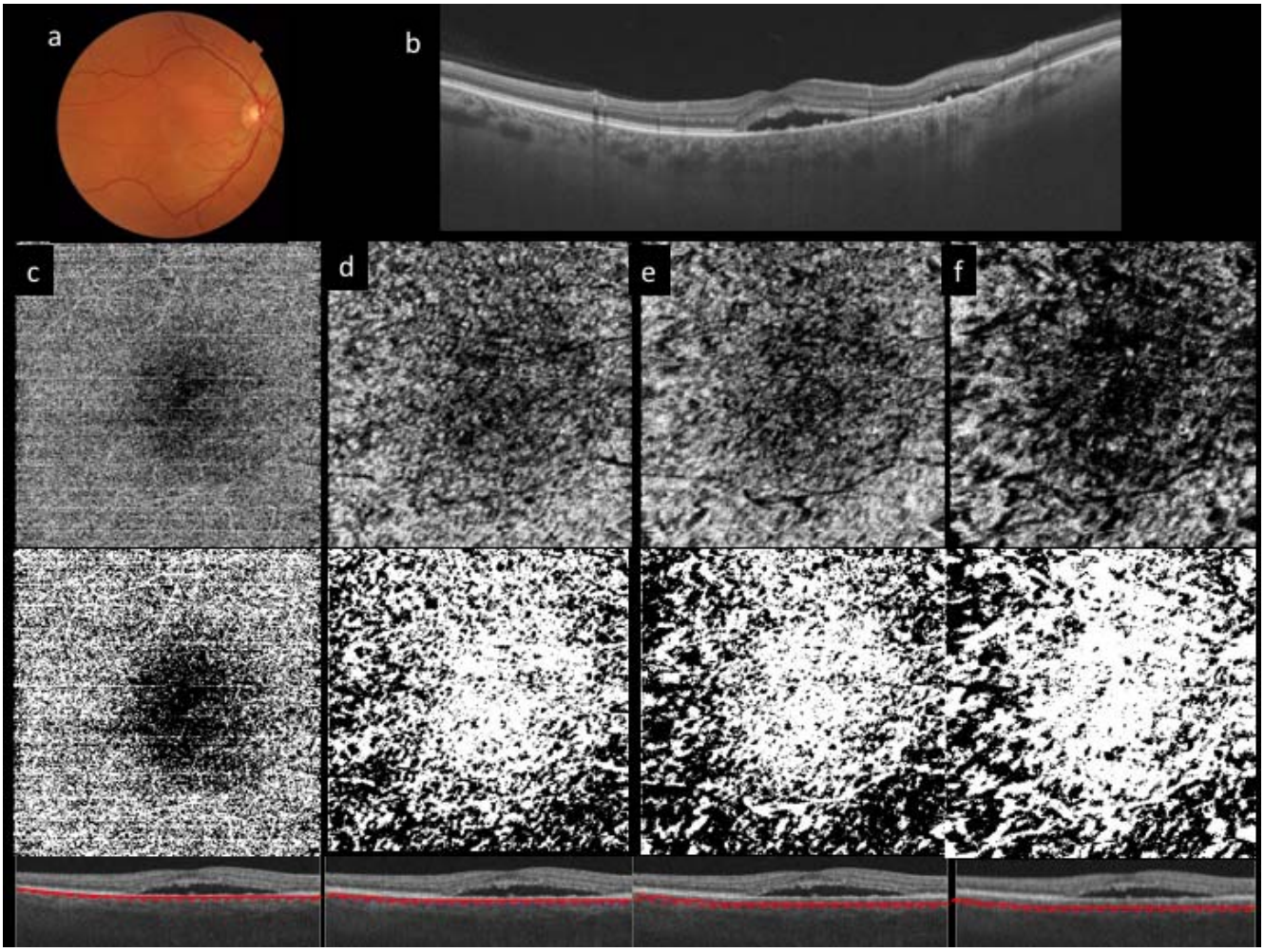

FIGURE 2. Representative images of the right eye of a 48-year-old man with chronic central serous chorioretinopathy. Compared with Figure 1 there is a prevalent dark pattern of the choroid, as vessels are more dilated, congested, and for this reason less outlined. (**a**) Fundus photograph. (**b**) Horizontal scan by SS-OCT. (**c**) *Upper*: OCTA image 4.5 × 4.5 mm of the microvasculature of the choriocapillaris 10.4-μm external to the Bruch's membrane; (**c**) *middle*: binarized image; (**c**) *bottom*: coregistered B scans showing the position of the segmentation lines. (**d**) *Upper*: OCTA image 4.5 × 4.5 mm of the choroid obtained positioning the segmentation line at 59.6 and 80.6 μm from the Bruch's membrane; (**d**) *middle*: binarized image; (**d**) *bottom*: coregistered B scans showing the position of the segmentation lines. (**e**) *Upper*: OCTA image 4.5 × 4.5 mm of the choroid obtained positioning the segmentation line at 80.6 and 119.6 μm from the Bruch's membrane; (**d**) *middle*: binarized image; (**d**) *bottom*: coregistered B scans showing the position of the segmentation lines. (**f**) *Upper*: OCTA image 4.5 × 4.5 mm of the choroid obtained positioning the segmentation line at 119.6 to 137.8 μm from the Bruch's membrane; (**f**) *middle*: binarized image; (**f**) *bottom*: coregistered B scans showing the position of the segmentation lines.

mean choroidal, Sattler and Haller layers is approximately 259.70 and 125 μm, respectively, in healthy subjects.[9,10] We then decided to select deep choroid at three different and consecutive Levels (L1, L2, and L3) positioning the segmentation lines between 59.6 and 80.6 μm, 80.6 and 119.6 μm, and 119.6 and 137.8 μm from the Bruch's membrane, respectively, in order to have representative slabs of the choroid (Figs. 1–4).

Measurement of Choroidal Vascular Flow Area

Each image was exported in jpg format and imported in the open access image analysis software Fiji.[11] In Fiji, each 320 × 320 pixels 8-bit images was binarized using the command path Image > Adjust > Threshold > Auto in order to calculate the percentage of black and white pixels. Binarization of an image was done by the Otsu method, which is an automatic threshold selection from gray-level histograms[12,13] (Figs. 5, 6). At SS-OCTA, choriocapillaris appears white while choroidal vessels are black. We assumed that the percentage of white or black pixels was an indirect measure of the choroidal vascular flow area of the choriocapillaris and deep choroid, respectively. The area of the portion of choroidal vascular flow was calculated in the pixel value. At angio-OCT, choriocapillaris is white while choroidal vessels under the choriocapillaris are black. For this reason, we calculate white pixel when we binarize the choriocapillaris gray-scale images and black pixel when we binarize the choroidal vessels gray-scale images. In the present study, the choroidal vascular flow area of the adopted images was defined as the percentage of the portion of white (Fig. 5) or black (Fig. 6) pixels against the whole scan area. The mean percentages of CC, L1, L2, L3, as well as the mean percentage of the values from L1 through L3 and from CC through L3 were calculated.

Statistical Analysis

Mann-Whitney *U* test was used to compare CSC, fellow, and control eyes each other. Wilcoxon test was used to compare

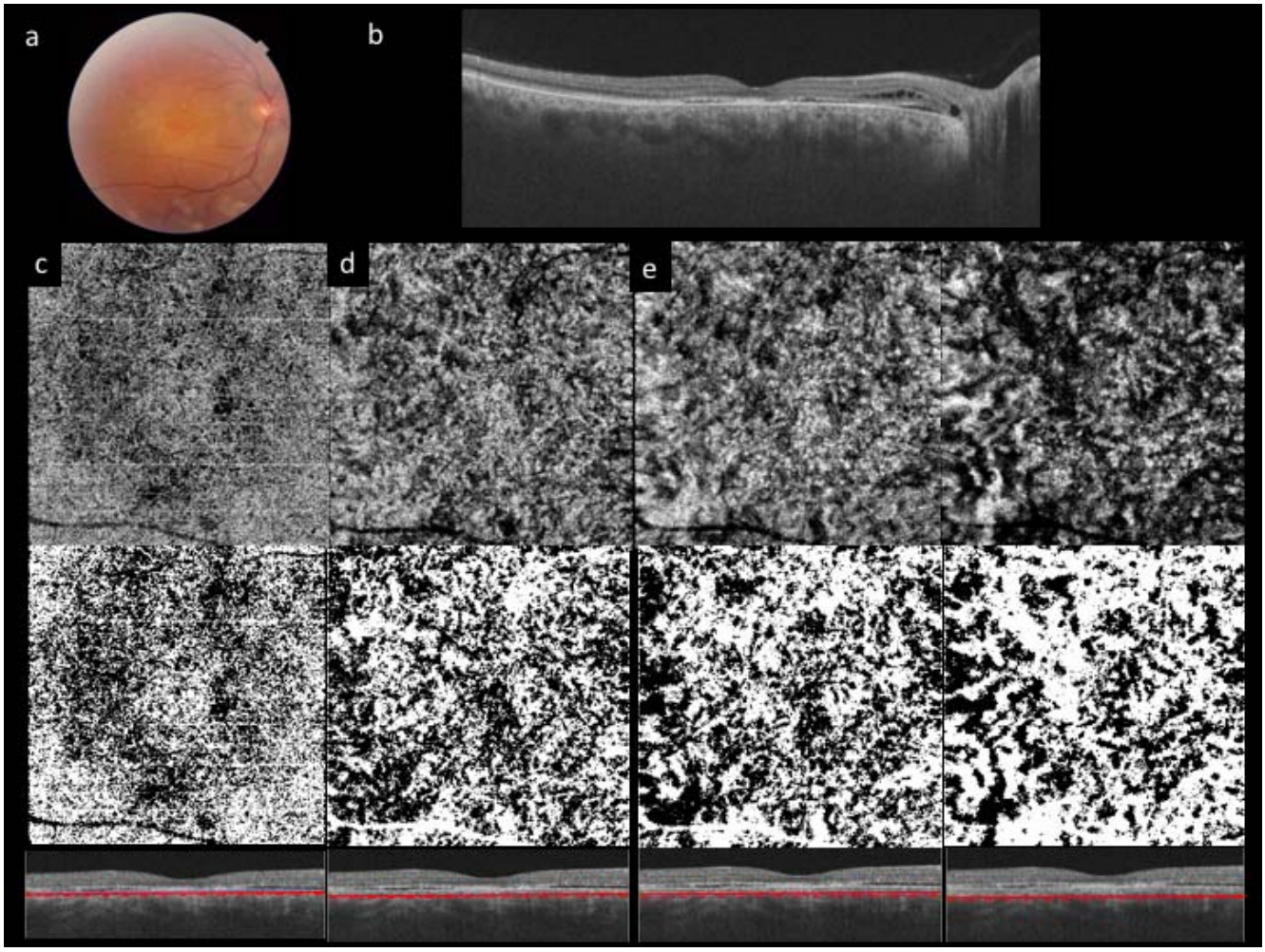

FIGURE 3. Representative images of the right eye of a 45-year-old man with chronic central serous chorioretinopathy. Compared with Figure 2 there is a very small amount of subretinal fluid but there is still a prevalent dark pattern of the choroid, as vessels are more dilated, congested and for this reason less outlined than healthy eyes. (**a**) Fundus photograph. (**b**) Horizontal scan by SS-OCT. (**c**) *Upper*: OCTA image 4.5 × 4.5 mm of the microvasculature of the choriocapillaris 10.4-μm external to the Bruch's membrane; (**c**) *middle*: binarized image; (**c**) *bottom*: coregistered B scans showing the position of the segmentation lines. (**d**) *Upper*: OCTA image 4.5 × 4.5 mm of the choroid obtained positioning the segmentation line at 59.6 and 80.6 μm from the Bruch's membrane; (**d**) *middle*: binarized image; (**d**) *bottom*: coregistered B scans showing the position of the segmentation lines. (**e**) *Upper*: OCTA image 4.5 × 4.5 mm of the choroid obtained positioning the segmentation line at 80.6 and 119.6 μm from the Bruch's membrane; (**d**) *middle*: binarized image; (**d**) *bottom*: coregistered B scans showing the position of the segmentation lines. (**f**) *Upper*: OCTA image 4.5 × 4.5 mm of the choroid obtained positioning the segmentation line at 119.6 to 137.8 μm from the Bruch's membrane; (**f**) *middle*: binarized image; (**f**) *bottom*: coregistered B scans showing the position of the segmentation lines.

values within groups. Statistical significance was set at P less than 0.05.

RESULTS

In this study, 19 eyes of 19 patients with CSC and 20 eyes of 10 healthy subjects were included. Fifteen patients had unilateral CSC and four patients had bilateral CSC. Central serous chorioretinopathy patients and control subjects were similar in age (53.11 ± 8.8 vs. 57.5 ± 8.4; $P = 0.8$) and axial length (23.2 ± 1.3 mm vs. 23.9 ± 1.3 mm; $P = 0.43$). There was no difference in sex distribution between the CSC patients and control subjects (18 men and 1 female versus 9 men and 1 female; $P = 0.6$). The mean subfoveal choroidal thickness of eyes with CSC (337.0 ± 57.93 μm) was significantly larger ($P < 0.0001$) compared with control eyes (211.2 ± 60.1 μm) (Table 1). Overall the choroidal vascular flow area was significantly higher in eyes with CSC than in control eyes (53.4 ± 5.8% vs. 49.45 ± 8.16%; $P = 0.0001$; Table 2). The choroidal vascular flow area at the level of the CC was significantly higher in eyes with CSC than in control eyes (50.97 ± 2.8% vs. 48.43 ± 1%; $P < 0.0001$). The choroidal vascular flow area at deeper choroidal levels (L1, L2, L3) (54.22 ± 6.3% vs. 49.80 ± 9.3%; $P = 0.0083$) was significantly higher in eyes with CSC than in control eyes (Table 2). Within the choroid of CSC patients choroidal vascular flow area of the CC was significantly lower than the deeper level (50.97 ± 2.8% vs. 54.22 ± 6.3%; $P = 0.025$) while there were no differences within the choroid of control eyes (Table 3). Unaffected fellow eyes ($n = 15$) and control eyes were similar in age ($P = 0.16$) and axial length ($P = 0.32$). The mean subfoveal choroidal thickness was larger in the unaffected fellow eyes (298.6 ± 101.9 μm) compared with the control eyes $P = 0.0001$. Overall, the choroidal vascular flow area was significantly higher in the unaffected fellow eyes with CSC than in control eyes (52.78 ± 6.3%; $P = 0.03$). The choroidal vascular flow area at the level of the CC was significantly higher in the unaffected fellow eye

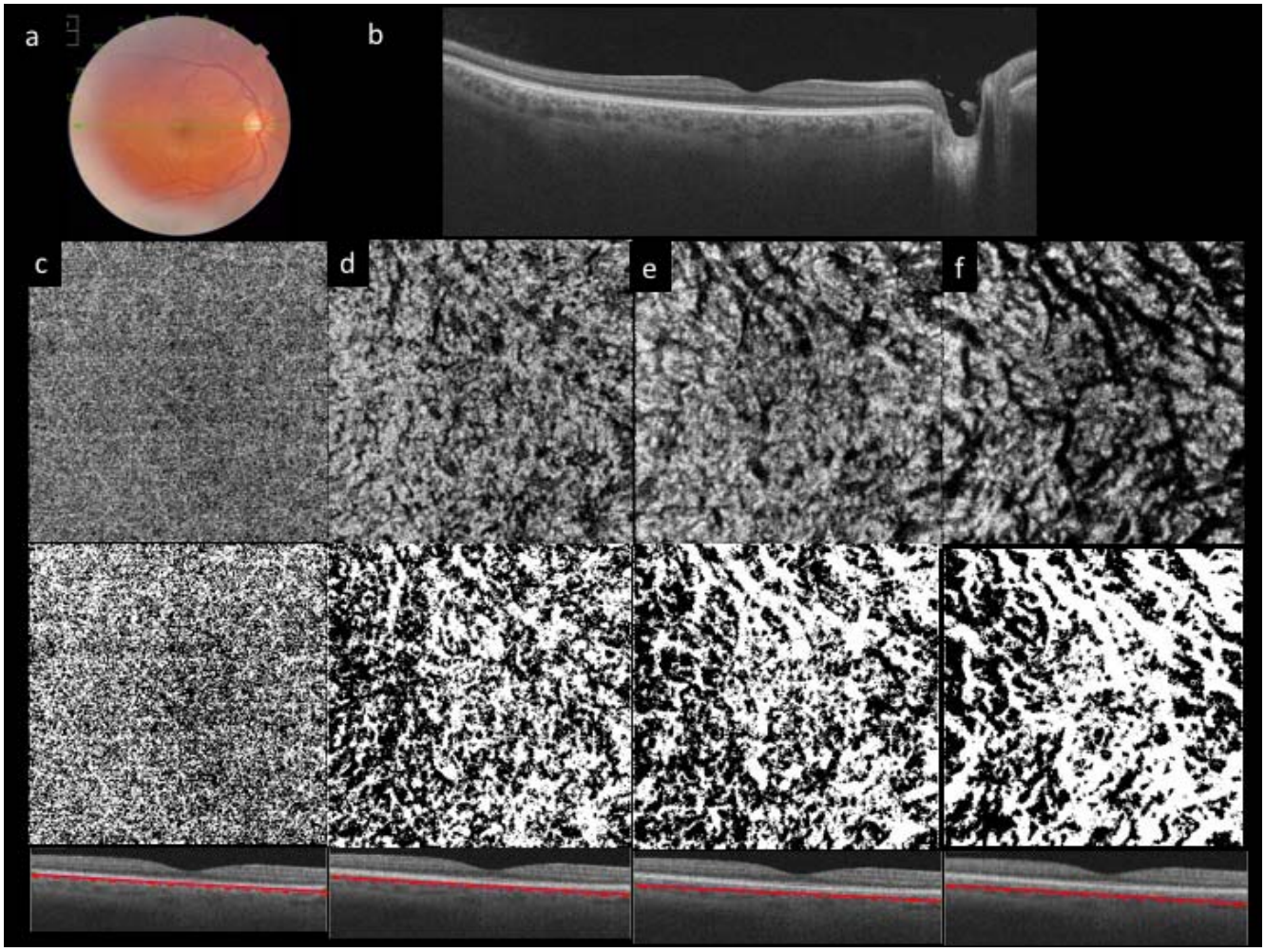

Figure 4. Representative images of the fellow right eye of a 48-year-old man with chronic central serous chorioretinopathy. Compared with Figures 2 and 3 there is no subretinal fluid but there is still a prevalent dark pattern of the choroid, as vessels are more dilated, congested and for this reason less outlined than healthy eyes. (**a**) Fundus photograph. (**b**) Horizontal scan by SS-OCT. (**c**) *Upper*: OCTA image 4.5 × 4.5 mm of the microvasculature of the choriocapillaris 10.4-μm external to the Bruch's membrane; (**c**) *middle*: binarized image; (**c**) *bottom*: coregistered B scans showing the position of the segmentation lines. (**d**) *Upper*: OCTA image 4.5 × 4.5 mm of the choroid obtained positioning the segmentation line at 59.6 and 80.6 μm from the Bruch's membrane; (**d**) *middle*: binarized image; (**d**) *bottom*: coregistered B scans showing the position of the segmentation lines. (**e**) *Upper*: OCTA image 4.5 × 4.5 mm of the choroid obtained positioning the segmentation line at 80.6 and 119.6 μm from the Bruch's membrane; (**d**) *middle*: binarized image; (**d**) *bottom*: coregistered B scans showing the position of the segmentation lines. (**f**) *Upper*: OCTA image 4.5 × 4.5 mm of the choroid obtained positioning the segmentation line at 119.6 to 137.8 μm from the Bruch's membrane; (**f**) *middle*: binarized image; (**f**) *bottom*: coregistered B scans showing the position of the segmentation lines.

(50.74 ± 0.9%; $P = 0.02$) than in control eyes (Table 4). Mean subfoveal choroidal thickness of unaffected eyes (298.6 ± 57.87 μm; $P = 0.06$) was not statistically significant different compared with CSC eyes. Overall, the choroidal vascular flow area of unaffected fellow eyes did not differ significantly from CSC eyes ($P = 0.7$), however the choroidal vascular flow area at the level of the CC was significantly higher in the CSC eyes ($P = 0.0009$) compared with unaffected fellow eyes (Table 5). There was no statistically significant correlation between the subfoveal choroidal thickness and the choroidal vascular flow area at the level of the microvasculature of the choroid at any level.

Discussion

In the present study, we evaluated the choroidal vascular flow area of CSC eyes using SS-OCT angiography imaging.

Optical coherence tomography angiography is a fast, easy, noninvasive, 3D imaging method to visualize intravascular flow at the microcirculation level. Optical coherence tomography angiography implementation further benefits from being paired with SS-OCT technology, given the high 100 kHz A-line rate, 1-μm wavelength light source, and deep signal penetration through the retina and choroid.[14–16] Furthermore, SS-OCT utilizes longer wavelength infrared light than conventional spectral-domain OCT, and therefore has improved penetration into tissue allowing a better visualization of the choroid. Optical coherence tomography angiography methods are generally based on quantification of motion contrast. In a practical implementation, ocular B-scan data may be scanned two or more times in the same location, and a calculation is performed across corresponding pixels in each frame or combination of frames in order to quantify the degree of motion contrast. This measure is then presumed to correspond to angiographic flow, as blood flow is the primary cause of signal change under normal imaging conditions after bulk

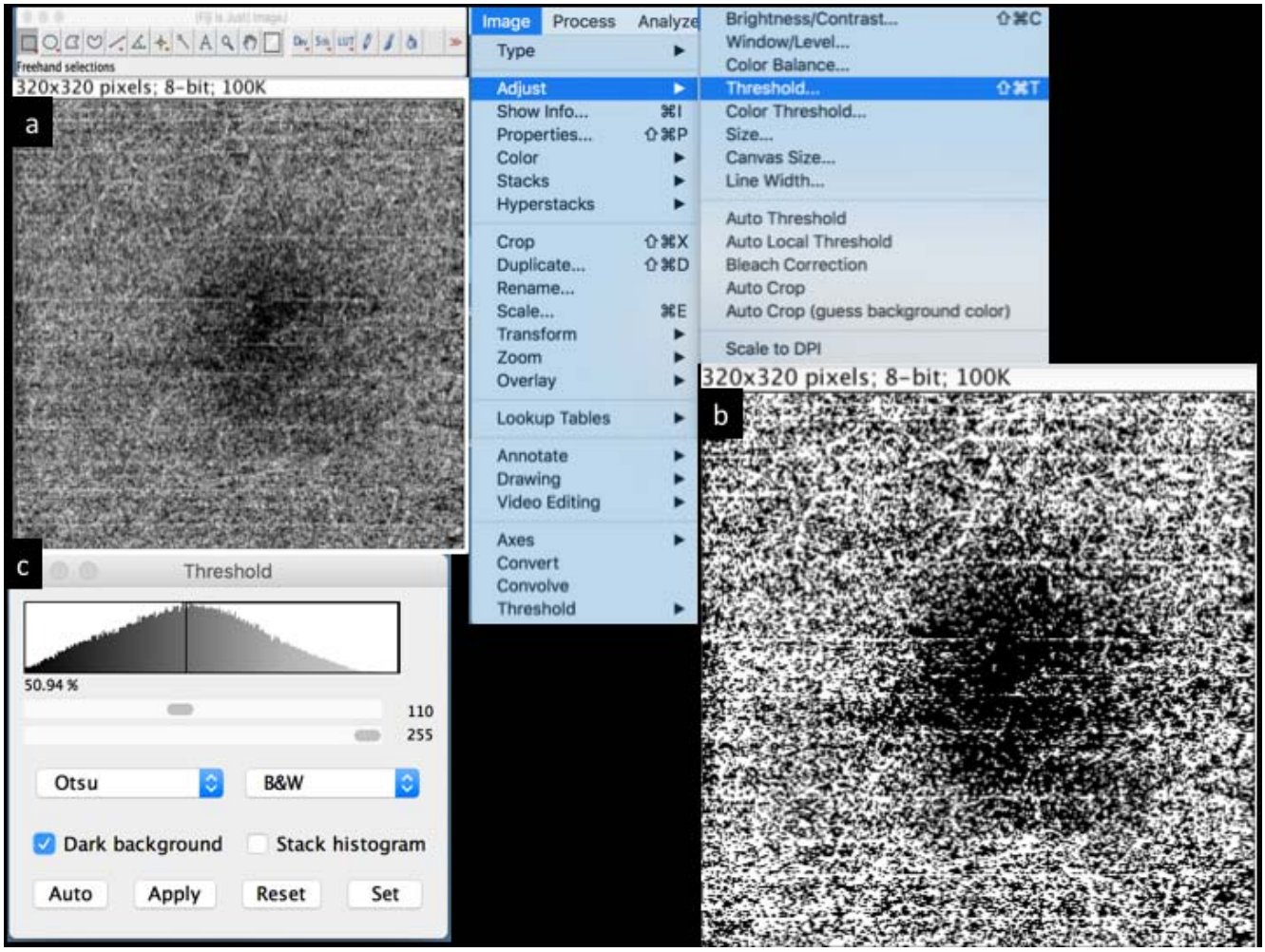

Figure 5. Procedure to calculate the white pixel percentage in CC image obtained automatically by the SS-OCTA software machine. Imported into Fiji software are 320 × 320 pixels 8-bit images (**a**); then image was binarized (**b**) using the command path Image > Adjust > Threshold > Auto in order to calculate the percentage of white black pixels (**c**) using the Otsu method.

motion has been accounted for. Some angiographic methods compute the differences between image frames, whereas others may compute the variance over an arbitrary number of frames.[14–16] In this paper, we used a SS-OCTA machine with a motion contrast measure using a ratio method, named OCTARA (OCT Angiography Ratio Analysis), where the full spectrum is kept intact and therefore the axial resolution is preserved.[4]

The results of our study demonstrated that the vascular flow area of the choroid is significantly larger in eyes with CSC as well as unaffected fellow eyes than in age-matched healthy control eyes. On the contrary we found no difference in the vascular flow area of the choroid between CSC eyes and unaffected fellow-eyes. Choroidal thickness was significantly higher in both CSC and unaffected fellow eyes compared with control eyes and no difference in choroidal thickness was found between CSC eyes and unaffected fellow eyes. Once again, our data confirm that the pathogenesis of the CSC is a consequence of a choroidal disease. However, our data showed also that there might be a different spatial distribution of the vascular flow within the choroid in CSC eyes depending to the depth. As a matter of fact, we found that the choroidal vascular flow area at the level of CC is significantly smaller compared with the deeper levels. On the contrary no differences were found within the choroid in the control eyes.

Table 1. Demography of 19 Eyes (19 Patients) With Central Serous Chorioretinopathy and 20 Healthy Eyes (10 Patients)

Value	CSC	Healthy	*P* Value
Age	53.11 ± 8.8	57.5 ± 8.4	0.8
AL, mm	23.2 ± 1.3	23.9 ± 1.3	0.3
Sex	18 m; 1 f	9 m; 1 f	0.6
SFCT	341.3 ± 64.93	211.2 6 ± 60.1	<0.0005

AL, axial length; f, female; SFCT, subfoveal choroidal thickness.

Table 2. Choroidal Vascular Flow Area in 19 Eyes With Central Serous Chorioretinopathy and 20 Healthy Eyes

Flow Area	Healthy, %	CSC, %	*P* Value
CC	48.43 ± 1.0	50.97 ± 2.8	<0.0001
L1 (59.8–80.6)	49.16 ± 5.5	49.99 ± 4.4	0.8
L2 (80.6–119.6)	48.14 ± 6.9	52.25 ± 2.5	0.1
L3 (119.6–137.8)	52.10 ± 13.63	60.43 ± 6.0	0.13
L1+L2+L3	49.80 ± 9.36	54.22 ± 6.3	0.0083
Total	49.45 ± 8.16	53.4 ± 5.8	0.0001

L, level; Total (CC+ L1+L2+L3).

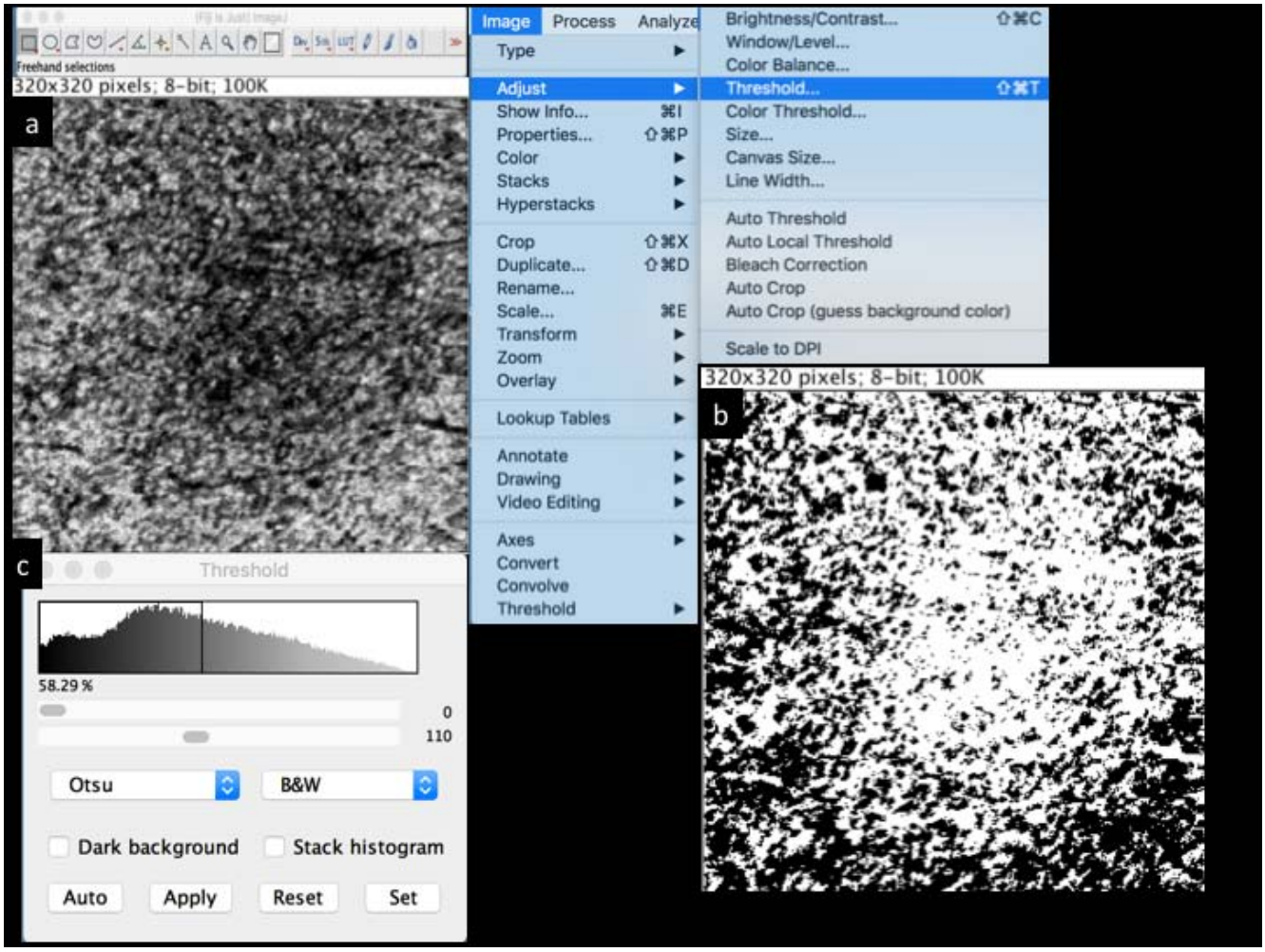

Figure 6. Procedure to calculate the black pixel percentage in Level 1 image obtained moving down the segmentation line at 59.6 and 80.6 μm from the Bruch's membrane. Imported into Fiji software are 320 × 320 pixels 8-bit images (**a**); then image was binarized (**b**) using the command path Image > Adjust > Threshold > Auto in order to calculate the percentage of black pixels by removing the tick dark background (**c**) using the Otsu method.

Although the etiology of CSC is still to be determined, previous studies using IGCA showed that choroid is primarily involved in the pathogenesis of the disease. Particularly choroidal vascular abnormalities of eyes with CSC, including delayed filling, vascular congestion, choroidal vascular hyperpermeability, and punctate hyperfluorescent spots[17–23] have been previously described, suggesting that the primary pathogenesis of CSC and subretinal fluid is choroidal vascular disturbance in presence of RPE defects and abnormalities.[24,25]

The flow rate (i.e., the volume of blood that passes a given point per unit time) is determined by pressure gradient and/or the size of the vessel. The peripheral resistance determines the direction of blood flow out of the choriocapillaris lobule. Because this resistance is usually lower in the peripheral collecting venules of the lobules than in adjacent lobular units, the blood moves into the veins rather than into contiguous capillaries.[26] Many reports showed that, contrarily to retinal blood flow, which has the intrinsic ability to maintain a relatively constant blood flow despite changes in perfusion pressure or size of the vessel[27–30] choroidal circulation is a passive vascular bed with a limited autoregulatory capacity.[27,28,31–37]

To the best of our knowledge, this is the first paper to investigate the choroidal vascular flow area using SS-OCT

Table 3. Comparison of the Choroidal Vascular Flow Area Within the Choriocapillaris Compared With the Deeper Level in 20 Healthy Eyes and 19 Eyes With Central Serous Chorioretinopathy

Flow Area	Healthy, %	*P* Value	CSC, %	*P* Value
CC	48.43 ± 1.0		50.97 ± 2.8	
L1 (59.8–80.6)	49.16 ± 5.5	0.5	49.99 ± 4.4	0.4
L2 (80.6–119.6)	48.14 ± 6.9	0.9	52.25 ± 2.5	0.1
L3 (119.6–137.8)	52.10 ± 13.63	0.2	60.43 ± 6.0	<0.0001
L1+L2+L3	49.80 ± 9.36	0.5	54.22 ± 6.3	0.025

Table 4. Choroidal Vascular Flow Area in 20 Healthy Eyes and 15 Unaffected Fellow Eyes

Flow Area	Healthy, %	Fellow, %	*P* Value
CC	48.43 ± 1.0	50.74 ± 0.9	0.02
L1 (59.8–80.6)	49.16 ± 5.53	49.17 ± 3.7	0.89
L2 (80.6–119.6)	48.14 ± 7.0	51.53 ± 1.8	0.03
L3 (119.6–137.8)	52.10 ± 13.63	61.16 ± 6.7	0.01
L1+L2+L3	49.80 ± 9.6	53.95 ± 6.8	0.03
Total	49.45 ± 8.16	52.78 ± 6.3	0.005

Table 5. Choroidal Vascular Flow Area in 19 Eyes Affected by Central Serous Chorioretinopathy and 15 Unaffected Fellow Eyes

Flow Area	CSC, %	Fellow, %	*P* Value
CC	50.97 ± 2.8	50.74 ± 0.90	0.0009
L1 (59.8–80.6)	49.99 ± 4.4	49.17 ± 3.7	0.7
L2 (80.6–119.6)	52.25 ± 2.5	51.53 ± 1.8	0.4
L3 (119.6–137.8)	60.43 ± 6.0	61.16 ± 6.7	0.8
L1+L2+L3	54.22 ± 6.3	53.95 ± 6.8	0.6
Total	53.4 ± 5.8	52.78 ± 6.3	0.17

angiography in patients affected by CSC. Previous authors tried to compare spectral-domain OCT angiography pattern with fluorescein and ICG angiography in CSC patients. They found significant textural changes of the choriocapillaris flow pattern with foci of ischemia surrounded by reactive choroidal hyperperfusion,[5] image pattern of high signal intensity in the layer of the choriocapillaris,[6] or failed to reveal altered flow pattern at the level of the choriocapillaris.[7] None of these authors, report the status of the vascular flow under the choriocapillaris probably as a consequence of the failure of the shorter wavelength of the spectral-domain machine to penetrate the choriocapillaris.

Previous authors investigated the vascular density of the choroid[13] using en-face SS-OCT. They demonstrated that vascular areas of the choroid were larger in eyes with CSC and unaffected fellow eyes than in age-matched healthy controls, both at the level of the microvasculature of the inner choroid and at the large choroidal vessel level.

Limitations of this study are related to the relatively small number of patients as well as the possible bias both in the acquisition of the exam and image processing. Scans might also contain artifact projection of the retinal vessels as well as potential segmentation errors when using the automated segmentation.[38] Furthermore, although we measured a significant part of the choroid, our results might be not representative of the changes in the whole choroid during CSC.

The "dark pattern" of the choroid, which might be an artifact, is indeed present regardless of the amount of fluid in CSC (Figs. 2, 3) as well as in fellow eyes (Fig. 4) but it is not present in healthy eyes (Fig. 1).

Our results confirm that the choroidal vascular flow area is larger at any level analyzed in CSC eyes compared with control eyes. However, within the choroid of eyes with CSC, there might be some differences in flow area between CC and deeper choroidal levels. This difference might be secondary to a compensatory mechanism of the choroid.

We hypothesize that following to an increased sensibility to vasoactive substances there might be a vasodilatation of part of the choroid and a relative vasoconstriction of the choriocapillaris in the attempt to compensate to the limited autoregulatory capacity of the choroid.

It is likely that the continue research in the field of OCT angiography technique will contribute to significantly improve our knowledge and understanding on the pathogenesis of CSC.

Acknowledgments

Disclosure: **M. Nicolò**, None; **R. Rosa**, None; **D. Musetti**, None; **M. Musolino**, None; **M. Saccheggiani**, None; **C.E. Traverso**, None

References

1. Piccolino FC, Borgia L. Central serous chorioretinopathy and indocyanine green angiography. *Retina*. 1994;14:231–242.
2. Cardillo Piccolino F, Rigault de la Longrais R, Ravera GB, et al. The foveal photoreceptor layer and visual acuity loss in central serous chorioretinopathy. *Am J Ophthalmol*. 2005; 139:87–99.
3. Yannuzzi LA. Central serous chorioretinopathy: a personal perspective. *Am J Ophthalmol*. 2010;149:361–363.
4. Stanga PE, Tsamis E, Papayannis A, Stringa F, Cole T, Jalil A. Swept-Source Optical Coherence Tomography Angio™ (Topcon Corp, Japan): technology review. *Dev Ophthalmol*. 2016; 56:13–17.
5. Teussink MM, Breukink MB, van Grinsven MJJP, et al. OCT angiography compared to fluorescein and indocyanine green angiography in chronic central serous chorioretinopathy. *Invest Ophthalmol Vis Sci*. 2015;56:5229–5237.
6. Chan SY, Wang Q, Wei WB, Jonas JB. Optical coherence tomographic angiography in central serous chorioretinopathy *Retina*. 2016;36:2051–2058.
7. Feucht N, Maier M, Lohmann CP, Reznicek L. OCT angiography findings in acute central serous chorioretinopathy ophthalmic surgery. *Ophthalmic Surg Lasers Imaging Retina*. 2016;47:322–327.
8. Daruich A, Matet A, Dirani A, et al. Central serous chorioretinopathy: recent findings and new physiopathology hypothesis. *Prog Retin Eye Res*. 2015;48:82–118.
9. Esmaeelpour M, Kajic V, Zabihian B, et al. Choroidal Haller's and Sattler's layer thickness measurement using 3-dimensional 1060-nm optical coherence tomography. *PLoS One*. 2014;9: e99690.
10. Esmaeelpour M, Ansari-Shahrezaei S, Glittenberg C, et al. Choroid, Haller's, and Sattler's layer thickness in intermediate age-related macular degeneration with and without fellow neovascular eyes. *Invest Ophthalmol Vis Sci*. 2014;55:5074–5080.
11. Schindelin J, Arganda-Carreras I, Frise E, et al. Fiji: an open-source platform for biological-image analysis. *Nat Methods*. 2012;9:676–682.
12. Otsu N. A threshold selection method from gray-level histograms. *IEEE Trans Syst Man Cybern*. 1979;9:62–66.
13. Kuroda Y, Ooto S, Yamashiro K, et al. Increased choroidal vascularity in central serous chorioretinopathy quantified using swept-source optical coherence tomography. *Am J Ophthalmol*. 2016;169:199–207.
14. Mariampillai A, Standish BA, Moriyama EH, et al. Speckle variance detection of microvasculature using swept-source optical coherence tomography. *Opt Lett*. 2008;33:1530–1532.
15. Jia Y, Tan O, Tokayer J, et al. Split-spectrum amplitude-decorrelation angiography with optical coherence tomography. *Opt Express*. 2012;20:4710–4725.
16. Huang Y, Zhang Q, Thorell MR, et al. Swept-source OCT angiography of the retinal vasculature using intensity differentiation-based optical microangiography algorithms. *Ophthalmic Surg Lasers Imaging Retina*. 2014;45:382–389.
17. Hayashi K, Hasegawa Y, Tokoro T. Indocyanine green angiography of central serous chorioretinopathy. *Int Ophthalmol*. 1986;9:37–41.
18. Guyer DR, Yannuzzi LA, Slakter JS, Sorenson JA, Ho A, Orlock D. Digital indocyanine green videoangiography of central serous chorioretinopathy. *Arch Ophthalmol*. 1994;112:1057–1062.
19. Prunte C. Indocyanine green angiographic findings in central serous chorioretinopathy. *Int Ophthalmol*. 1995;19:77–82.
20. Prunte C, Flammer J. Choroidal capillary and venous congestion in central serous chorioretinopathy. *Am J Ophthalmol*. 1996;121:26–34.
21. Giovannini A, Scassellati-Sforzolini B, D'Altobrando E, Mariotti C, Rutili T, Tittarelli R. Choroidal findings in the course of idiopathic serous pigment epithelium detachment detected

by indocyanine green videoangiography. *Retina*. 1997;17: 286–293.

22. Iida T, Kishi S, Hagimura N, Shimizu K. Persistent and bilateral choroidal vascular abnormalities in central serous chorioretinopathy. *Retina*. 1999;19:508–512.
23. Tsujikawa A, Ojima Y, Yamashiro K, et al. Punctate hyperfluorescent spots associated with central serous chorioretinopathy as seen on indocyanine green angiography. *Retina*. 2010;30:801–809.
24. Donald J, Gass M. Pathogenesis of disciform detachment of the neuroepithelium: II. Idiopathic central serous choroidopathy. *Am J Ophthalmol*. 1967;63:587–615.
25. Yao XY, Marmor MF. Induction of serous retinal detachment in rabbit eyes by pigment epithelial and choriocapillary injury. *Arch Ophthalmol*. 1992;110:541–546.
26. Fryczkowski AW. Anatomical and functional choroidal lobuli. *Int Ophthalmol*. 1994;18:131–134.
27. Bill A. Circulation in the eye. In: Renkin EM, Michel CC, eds. *Handbook of Physiology: The Cardiovascular System*. Vol 2. Baltimore: Waverly Press; 1984:1001–1034.
28. Ffytche TJ, Bulpitt CJ, Kohner EM, et al. Effect of changes in intraocular pressure on the retinal microcirculation. *Br J Ophthalmol*. 1974;58:514–522.
29. Riva CE, Grunwald JE, Petrig BL. Autoregulation of human retinal blood flow. *Invest Ophthalmol Vis Sci*. 1986;27:1706–1712.
30. Robinson F, Riva CE, Grunwald JE, et al. Retinal blood flow in response to an acute increase in blood pressure. *Invest Ophthalmol Vis Sci*. 1986;27:722–726.
31. Alm A, Bill A. Ocular and optic nerve blood flow at normal and increased intraocular pressure in monkeys (Macaca irus): a study with radioactively labelled microspheres including flow determinations in brain and some other tissues. *Exp Eye Res*. 1973;15:15–29.
32. Alm A, Bill A. The oxygen supply to the retina: II. Effects of high intraocular pressure and of increased arterial carbon dioxide tension on uveal and retinal blood flow in cats: a study with radioactively labelled microspheres including flow determinations in brain and some other tissues. *Acta Physiol Scand*. 1972;84:306–319.
33. Alm A, Bill A. Blood flow and oxygen extraction in the cat uvea at normal and high intraocular pressures. *Acta Physiol Scand*. 1970;80:19–28.
34. Bill A. Intraocular pressure and blood flow through the uvea. *Arch Ophthalmol*. 1962;67:336–348.
35. Friedman E. Choroidal blood flow: pressure-flow relationships. *Arch Ophthalmol*. 1970;83:95–99.
36. Yu DY, Alder VA, Cringle SJ, Brown MJ. Choroidal blood flow measured in the dog eye in vivo and in vitro by local hydrogen clearance polarography: validation of a technique and response to raised intraocular pressure. *Exp Eye Res*. 1988; 46:289–303.
37. Nickla DL, Wallman J. The multifunctional choroid. *Prog Retin Eye Res*. 2010;29:144–168.
38. Lupidi M, Coscas F, Cagini C, et al. Automated quantitative analysis of retinal microvasculature in normal eyes on optical coherence tomography angiography. *Am J Ophthalmol*. 2016; 169:9–23.

Investigative Ophthalmology & Visual Science